SUPPLEMENTARY MATERIAL

S1 – FORMULA DERIVATION

COWAN'S MODEL

Cowan (1968) estimated that the eddy diffusivity scaled with the velocity within the canopy:

$$\frac{\frac{K_M(z)}{\cancel{H}}}{U(z)} = \frac{\frac{K_M(H_c)}{\cancel{H}}}{U_H} \;, \quad for\ z \leq H_c$$

$$K_M(z) = K_M(H_c)\frac{U(z)}{U_H} \tag{S1}$$

Substituting (S1) into the force balance equation (8) in the main text gives:

$$\frac{d}{dz}\left(K_M(z)\frac{dU(z)}{dz}\right) = \frac{c_d a}{2}U(z)^2$$

$$\frac{d}{dz}\left(\frac{K_M(H_c)}{U_H}U(z)\frac{dU(z)}{dz}\right) = \frac{c_d a}{2}U(z)^2$$

$$U(z)\frac{d^2U(z)}{dz^2} + \left(\frac{dU(z)}{dz}\right)^2 = \frac{c_d a}{2}\frac{U_H}{K_M(H_c)}U(z)^2 \tag{S2}$$

This differential equation doesn't have a canonical solution, unlike Inoue (1963). The one proposed by Cowan is:

$$U(z) = U_H\left(\frac{\sinh\left(\sqrt{c_d a\frac{U_H}{K_M(H_c)}}\,z\right)}{\sinh\left(\sqrt{c_d a\frac{U_H}{K_M(H_c)}}\,H_c\right)}\right)^{\frac{1}{2}} \tag{S3}$$

To simplify the forthcoming analysis we will use Cowan's substitution of $\beta_{cw} = \sqrt{C_d a\frac{U_H}{K_M(H_c)}}$. From (S3) it follows that the first and second derivates are:

$$\frac{dU(z)}{dz} = \frac{U_H}{\sqrt{\sinh(\beta_{cw}H_c)}}\frac{\beta_{cw}\cosh(\beta_{cw}z)}{2\sqrt{\sinh(\beta_{cw}z)}} \tag{S4}$$

$$\frac{d^2U(z)}{dz^2} = \frac{U_H}{\sqrt{\sinh(\beta_{cw}H_c)}}\frac{{\beta_{cw}}^2}{2}\left(\sqrt{\sinh(\beta_{cw}z)} - \frac{(\cosh(\beta_{cw}z))^2}{2\left(\sqrt{\sinh(\beta_{cw}z)}\right)^3}\right) \tag{S5}$$

Equations (S3), (S4), and (S5) allow us to interrogate whether Cowan's solution satisfies the force balance equation (S2) imposed by his assumption of the eddy diffusivity (S1). The check is presented below:

$$U_H\left(\frac{\sinh(\beta_{cw}z)}{\sinh(\beta_{cw}H_c)}\right)^{\frac{1}{2}}.\frac{U_H}{\sqrt{\sinh(\beta_{cw}H_c)}}\frac{{\beta_{cw}}^2}{2}\left(\sqrt{\sinh(\beta_{cw}z)} - \frac{(\cosh(\beta_{cw}z))^2}{2\left(\sqrt{\sinh(\beta_{cw}z)}\right)^3}\right)$$
$$+\left(\frac{U_H}{\sqrt{\sinh(\beta_{cw}H_c)}}\frac{\beta_{cw}\cosh(\beta_{cw}z)}{2\sqrt{\sinh(\beta_{cw}z)}}\right)^2 = {\beta_{cw}}^2{U_H}^2\left(\frac{\sinh(\beta_{cw}z)}{\sinh(\beta_{cw}H_c)}\right)$$

$$\frac{{\beta_{cw}}^2 {U_H}^2}{\sinh(\beta_{cw} H_c)} \frac{\sqrt{\sinh(\beta_{cw} z)}}{2} \left(\sqrt{\sinh(\beta_{cw} z)} - \frac{(\cosh(\beta_{cw} z))^2}{2\left(\sqrt{\sinh(\beta_{cw} z)}\right)^3} \right) + \frac{{\beta_{cw}}^2 {U_H}^2}{\sinh(\beta_{cw} H_c)} \frac{(\cosh(\beta_{cw} z))^2}{4 \sinh(\beta_{cw} z)} = \frac{{\beta_{cw}}^2 {U_H}^2}{\sinh(\beta_{cw} H_c)} \frac{\sinh(\beta_{cw} z)}{2}$$

$$\frac{\sinh(\beta_{cw} z)}{2} - \frac{(\cosh(\beta_{cw} z))^2}{4\left(\sqrt{\sinh(\beta_{cw} z)}\right)^2} + \frac{(\cosh(\beta_{cw} z))^2}{4 \sinh(\beta_{cw} z)} = \frac{\sinh(\beta_{cw} z)}{2}$$

$$\frac{\sinh(\beta_{cw} z)}{2} = \frac{\sinh(\beta_{cw} z)}{2}$$

We can see that the proposed velocity (S3) satisfies the force balance equation (S2) developed by the assumption regarding eddy diffusivity (S1). To derive the relationship between d_0 and z_{0m} the CSL velocity gradient at H_c is calculated from (S4):

$$\frac{dU(H_c)}{dz} = \frac{U_H}{\sqrt{\sinh(\beta_{cw} H_c)}} \frac{\beta_{cw} \cosh(\beta_{cw} H_c)}{2\sqrt{\sinh(\beta_{cw} H_c)}} = \frac{\beta_{cw} U_H}{2 \tanh(\beta_{cw} H_c)} \tag{S6}$$

Equating the velocity gradient at H_c given by the CSL, equation (S6) with the velocity gradient generated by the ISL at H_c, and expanding the definition of β_{cw} gives:

$$\frac{\beta_{cw} U_H}{2 \tanh(\beta_{cw} H_c)} = \frac{u_*}{k(H_c - d_0)}$$

$$U_H \sqrt{c_d a \frac{U_H}{K_M(H_c)}} = \frac{2u_*}{k(H_c - d_0)} \tanh\left(\sqrt{c_d a \frac{U_H}{K_M(H_c)}} H_c \right)$$

$$\frac{k(H_c - d_0)}{2u_*} U_H \sqrt{c_d a \frac{U_H}{K_M(H_c)}} = \tanh\left(\sqrt{c_d a \frac{U_H}{K_M(H_c)}} H_c \right) \tag{S7}$$

Using the relationship that was shown in the main text equation (S14) $K_M(H_c)$ for we get:

$$\frac{k(H_c - d_0)}{2\beta} \sqrt{\frac{c_d a}{\beta k(H_c - d_0)}} = \tanh\left(\sqrt{\frac{c_d a}{\beta k(H_c - d_0)}} H_c \right)$$

$$\frac{k H_c \left(1 - \frac{d_0}{H_c}\right)}{2\beta} \sqrt{\frac{c_d a}{\beta k H_c \left(1 - \frac{d_0}{H_c}\right)}} = \tanh\left(\sqrt{\frac{c_d a {H_c}^2}{\beta k H_c \left(1 - \frac{d_0}{H_c}\right)}} \right)$$

$$\frac{k \left(1 - \frac{d_0}{H_c}\right)}{2\beta} \sqrt{\frac{c_d a H_c}{\beta k \left(1 - \frac{d_0}{H_c}\right)}} = \tanh\left(\sqrt{\frac{c_d a H_c}{\beta k \left(1 - \frac{d_0}{H_c}\right)}} \right) \tag{S8}$$

It is not possible to simplify the equation further given the approach utilized. We use the relationship derived for Inoue. Using the relationship derived from the velocity matching approach in the text equation (15), we see that z_{0m} can be written as;

$$\frac{z_0}{H_c} e^{\frac{k}{\beta}} = 1 - \frac{d_0}{H_c}$$

$$\frac{k\frac{z_0}{H_c}e^{\frac{k}{\beta}}}{2\beta}\sqrt{\frac{c_d a H_c}{\beta k\frac{z_0}{H_c}e^{\frac{k}{\beta}}}} = \tanh\left(\sqrt{\frac{c_d a H_c}{\beta k\frac{z_0}{H_c}e^{\frac{k}{\beta}}}}\right)$$

Thom's Model

Thom (1971) assumed that the eddy diffusivity within the canopy was constant. This allows the force balance relationship shown in the main text equation (S14):

$$K_M\frac{d}{dz}\left(\frac{dU(z)}{dz}\right) = c_d a U(z)^2 \tag{S9}$$

This differential equation doesn't have a canonical solution, unlike Inoue (1963). The one proposed by Cowan is:

The solution given by Thom is of the form:

$$U(z) = \frac{U_H}{\left\{1+\alpha\left(1-\frac{z}{H_c}\right)\right\}^2} \tag{S10}$$

The first and second derivates generated by the solution proposed by Thom is:

$$\frac{dU(z)}{dz} = \frac{2\alpha}{H_c}\frac{U_H}{\left\{1+\alpha\left(1-\frac{z}{H_c}\right)\right\}^3} \tag{S11}$$

$$\frac{d^2U(z)}{dz^2} = \frac{6\alpha^2}{{H_c}^2}\frac{U_H}{\left\{1+\alpha\left(1-\frac{z}{H_c}\right)\right\}^4} = \frac{6\alpha^2 U(z)^2}{U_H {H_c}^2} \tag{S12}$$

Substituting to the velocity derivatives relationships here we get;

$$K_M\frac{6\alpha^2 U(z)^2}{U_H {H_c}^2} = c_d a U(z)^2$$

$$\frac{6\alpha^2}{U_H {H_c}^2} = \frac{c_d a}{K_M}$$

$$\alpha = \sqrt{\frac{U_H {H_c}^2 c_d a}{6K_M}} \tag{S13}$$

Thom's simplifying assumption of constant eddy diffusivity up to H_c allows us to use the eddy diffusivity calculated from the ISL using dimensional arguments. In the ISL, the length-scale is the distance from the (vertically translated) surface and the velocity scale is u_*. So, the diffusivity at H_c, using k as the proportionality constant, can be written as:

$$K_M(H_c) = u_* k(H_c - d_0) \tag{S14}$$

Using this identity we get:

$$\alpha = \sqrt{\frac{U_H {H_c}^2 c_d a}{6u_* k(H_c - d_0)}}$$

$$\alpha = \sqrt{\frac{c_d a H_c}{6\beta k\left(1 - \frac{d_0}{H_c}\right)}} \tag{S15}$$

This allows us to write Thom's velocity model in terms of the non-dimensional parameters that the other models use. So the velocity profile becomes:

$$U(z) = \frac{U_H}{\left\{1 + \sqrt{\frac{c_d a H_c}{6\beta k\left(1 - \frac{d_0}{H_c}\right)}}\left(1 - \frac{z}{H_c}\right)\right\}^2} \tag{S16}$$

By velocity derivative matching we get the following answer:

$$\frac{2\alpha}{H_c}\frac{U_H}{\left\{1 + \alpha\left(1 - \frac{H_c}{H_c}\right)\right\}^3} = \frac{u_*}{k(H_c - d_0)}$$

$$\frac{(H_c - d_0)}{H_c} = \frac{\beta}{2\alpha k}$$

$$1 - \frac{d_0}{H_c} = \frac{\beta}{2\alpha k} \tag{S17}$$

Substituting the value for the alpha from (S15) we get;

$$1 - \frac{d_0}{H} = \frac{\beta}{2\sqrt{\frac{c_d a H_c}{6\beta k\left(1 - \frac{d_0}{H_c}\right)}}k}$$

$$\sqrt{\left(1 - \frac{d_0}{H_c}\right)} = \sqrt{\frac{\beta^2}{\frac{4k^2 c_d a H_c}{6\beta k}}}$$

$$\sqrt{\left(1 - \frac{d_0}{H_c}\right)} = \sqrt{\frac{3\beta^3}{2 c_d a H_c k}}$$

$$\frac{d_0}{H_c} = 1 - \frac{3\beta^3}{2 c_d a H_c k} \tag{S18}$$

This result is very similar to Inoue's with the difference of 0.5. This can be understood due to their insistence having a something constant through the canopy, in Inoue's case it was the mixing length and in Thom's it was the diffusivity.

WANG'S MODEL

All of the models discussed till can be used only in dense canopies. This is not the case with Wang (2012) who modelled the effect of the ground in influencing the wind velocity profile in the CSL within the sparse canopies. The eddy diffusivity to satisfy this condition is parameterized as:

$$K_M(z) = kzs_h u_* \tag{S19}$$

This diffusivity is the same as in the ISL, with the exception of s_h. s_h represents the effect of canopy elements on the eddy length scale. The force balance equation (S14) becomes:

$$\frac{d}{dz}\left(kzs_h u_* \frac{dU(z)}{dz}\right) = C_L a U(z) U_H \tag{S20}$$

Where the right hand side has been linearized and the effect of that linearization has been taken up in the transformation of drag coefficient into C_L. This makes the analytical solution:

$$U(z) = C_1 I_0\left(2\sqrt{\frac{C_L a U_H z}{k s_h u_*}}\right) - C_2 K_0\left(2\sqrt{\frac{C_L a U_H z}{k s_h u_*}}\right) \tag{S21}$$

Here, modified Bessel functions of the first ($I_x(*)$) and second kind ($K_x(*)$), where x is the order of the Bessel function and the rest of the constants are;

$$C_1 = \frac{U_H}{I_0\left(2\sqrt{\frac{C_L a U_H H_c}{k s_h u_*}}\right) + z_{0gr} K_0\left(2\sqrt{\frac{C_L a U_H H_c}{k s_h u_*}}\right)}$$

$$C_2 = C_1 z_{0gr}$$

$$z_{0gr} = \frac{I_0\left(2\sqrt{\frac{C_L a U_H z_{0g}}{k s_h u_*}}\right)}{K_0\left(2\sqrt{\frac{C_L a U_H z_{0g}}{k s_h u_*}}\right)} = \frac{I_0\left(2\sqrt{\frac{C_L a z_{0g}}{k s_h \beta}}\right)}{K_0\left(2\sqrt{\frac{C_L a z_{0g}}{k s_h \beta}}\right)}$$

The parameterisation of the ground roughness is done by a roughness length for momentum that characterizes the ground surface z_{0g}. Now using the velocity gradient matching at the canopy height, we get;

$$\frac{u_*}{k(H_c - d_0)} = C_1\sqrt{\frac{C_L a U_H}{k s_h u_* H_c}}\left\{I_1\left(2\sqrt{\frac{C_L a U_H H_c}{k s_h u_*}}\right) + z_{0gr} K_1\left(2\sqrt{\frac{C_L a U_H H_c}{k s_h u_*}}\right)\right\}$$

$$\frac{u_*}{C_1 k\sqrt{\frac{C_L a U_H}{k s_h u_* H_c}}\left\{I_1\left(2\sqrt{\frac{C_L a U_H H_c}{k s_h u_*}}\right) - z_{0gr} K_1\left(2\sqrt{\frac{C_L a U_H H_c}{k s_h u_*}}\right)\right\}} = (H_c - d_0)$$

$$d_0 = H_c - \frac{u_*}{C_1 k\sqrt{\frac{C_L a U_H}{k s_h u_* H_c}}\left\{I_1\left(2\sqrt{\frac{C_L a U_H H_c}{k s_h u_*}}\right) - z_{0gr} K_1\left(2\sqrt{\frac{C_L a U_H H_c}{k s_h u_*}}\right)\right\}}$$

$$d_0 = H_c - \frac{u_*\left\{I_0\left(2\sqrt{\frac{C_L a U_H H_c}{k s_h u_*}}\right) + z_{0gr} K_0\left(2\sqrt{\frac{C_L a U_H H_c}{k s_h u_*}}\right)\right\}}{U_H k\sqrt{\frac{C_L a U_H H_c}{k s_h u_*}}\left\{I_1\left(2\sqrt{\frac{C_L a U_H H_c}{k s_h u_*}}\right) - z_{0gr} K_1\left(2\sqrt{\frac{C_L a U_H H_c}{k s_h u_*}}\right)\right\}}$$

$$d_0 = H_c - \frac{\beta\left\{I_0\left(2\sqrt{\frac{C_L a H_c}{k s_h \beta}}\right) + z_{0gr} K_0\left(2\sqrt{\frac{C_L a H_c}{k s_h \beta}}\right)\right\}}{k\sqrt{\frac{C_L a}{k s_h \beta H_c}}\left\{I_1\left(2\sqrt{\frac{C_L a H_c}{k s_h \beta}}\right) - z_{0gr} K_1\left(2\sqrt{\frac{C_L a H_c}{k s_h \beta}}\right)\right\}}$$

$$\frac{d_0}{H} = 1 - \frac{\beta\left\{I_0\left(2\sqrt{\frac{C_L a H_c}{k s_h \beta}}\right) + z_{0gr} K_0\left(2\sqrt{\frac{C_L a H_c}{k s_h \beta}}\right)\right\}}{k\sqrt{\frac{C_L a H_c}{k s_h \beta}}\left\{I_1\left(2\sqrt{\frac{C_L a H_c}{k s_h \beta}}\right) - z_{0gr} K_1\left(2\sqrt{\frac{C_L a H_c}{k s_h \beta}}\right)\right\}} \tag{S22}$$

S2 – DIRECTIONAL DEPENDENCE

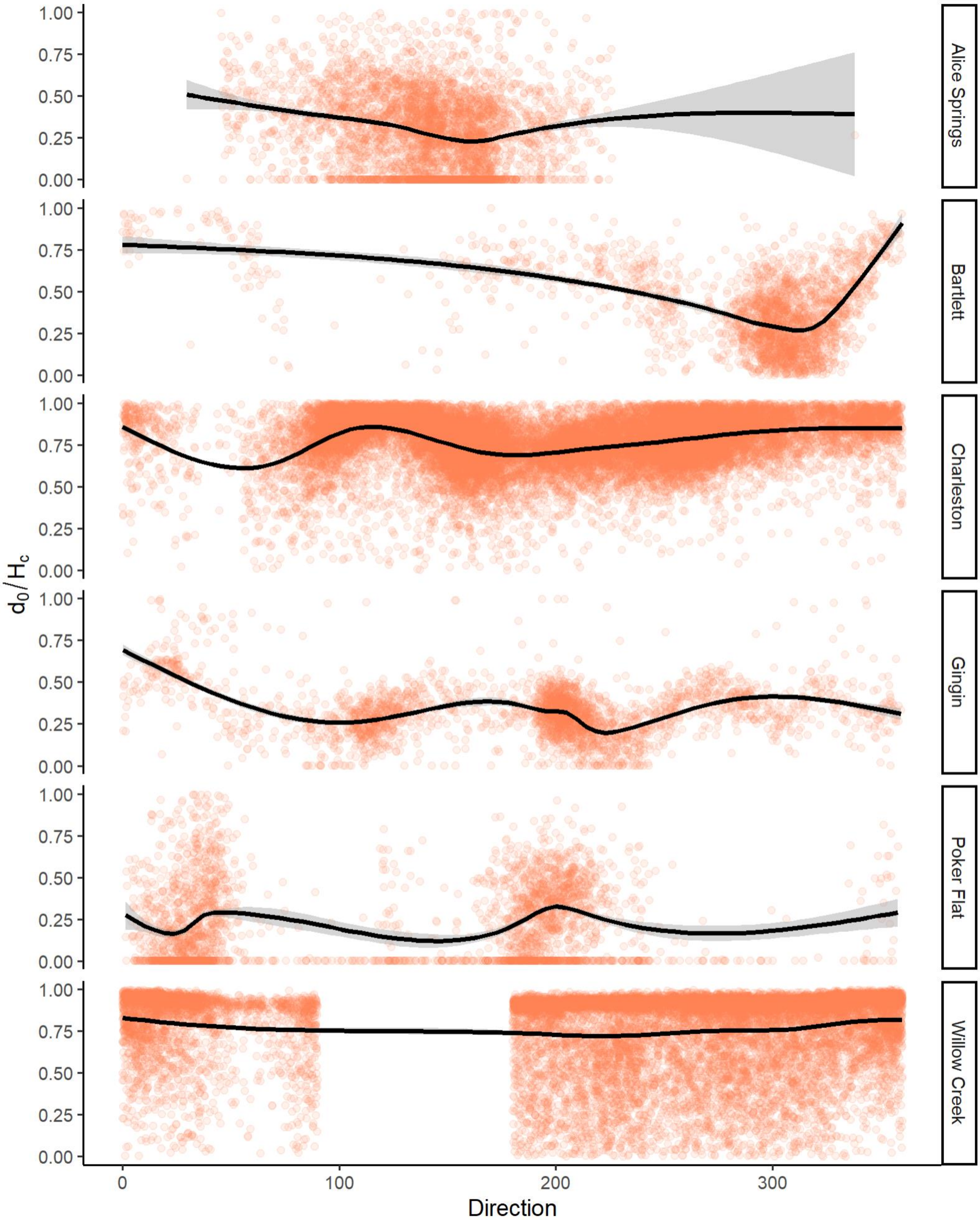

FIGURE S1: DIRECTIONAL DEPENDENCE OF EACH SITE. EVERY NEUTRAL HALF AN HOUR VALUE OF $\frac{d_0}{H_C}$ IS PLOTTED AS A POINT AGAINST THE MEAN DIRECTION OF FLOW FOR THAT HALF HOUR. THE BLACK LINE REPRESENTS A LOESS SMOOTHING FUNCTION WITH THE 95TH PERCENT CONFIDENCE INTERVALS REPRESENTED BY GREY BARS APPLIED TO SHOW THE DIRECTIONAL DEPENDENCE OF $\frac{d_0}{H_C}$.

S3 – ROBUSTNESS OF METHODS UTILIZED

There are different methods employed at different sites to derive d_0 and z_{0m} depending on whether the sites have one or more $U(z)$ measurements above H_c. As stated in Figure 2, if they have one, then d_0 is calculated using numerical derivative of Equation (2) and then z_{0m} from Equation (21). Whereas if they have more than one above H_c, then a least square methods is employed on Equation (3) to calculate both d_0 and z_{0m} simultaneously.

To make sure that both these estimates are comparable to each other, the following sense checks are performed:

1. d_0 is calculated using numerical derivatives at 3 heights using combination of 2 out of the 3 velocity measurements; this is compared with the least squares estimate of d_0 using all 3 velocity measurements at the same time step, at Gingin. As can be seen in the Figure S2, that while the estimates of d_0 from the two methods may not be the same (potentially due to z-dependence of the flux profile relationship within the RSL), they are highly correlated. This suggests i) that the variation can be estimated independently of the variation in z_{0m}, ii) there is variation in estimates of d_0 despite the method employed, and iii) they variation is highly correlated.

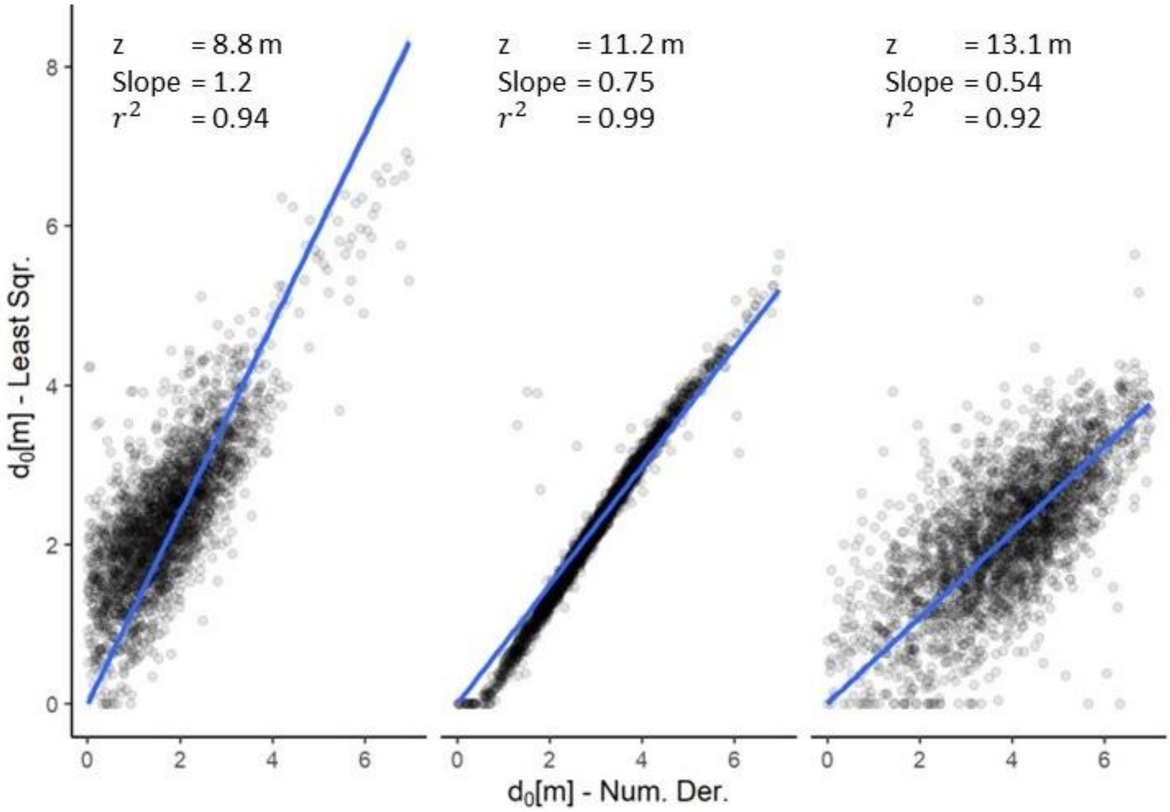

FIGURE S2: NUMERICAL DERIVATIVE (Y-AXIS) AND NLS d_0 COMPARISON FOR THREE DIFFERENT HEIGHTS (GIVEN AS 3 DIFFERENT PANELS) FOR GINGIN. THE TEXT FOR EACH PANEL SHOWS THE HEIGHT AT WHICH THE NUMERICAL DERIVATIVE WAS ANALYZED (Z), THE SLOPE OF THE X~Y RELATIONSHIP (INDICATED WITH A BLUE LINE), AND THE r^2 OF THAT RELATIONSHIP.

2. At sites with more than 1 wind speed sensor above H_c, z_{0m} is calculated using the least squared method with a variable d_0 and the mean $\overline{d_0}$. As can be seen in Figure S3, the two values are highly correlated and the variation in z_{0m} can be said to be captured independently of the variation in d_0.

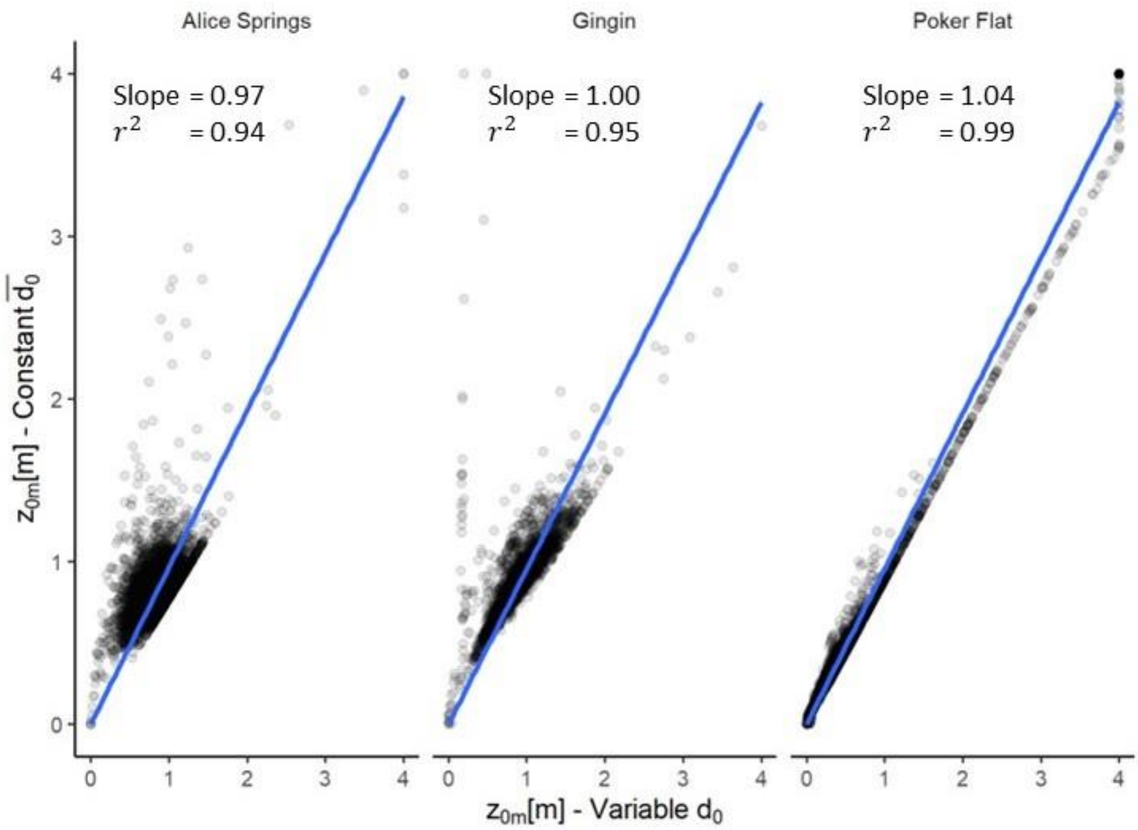

FIGURE S3: COMPARISON OF z_{0m} FROM USING FIXED d_0 (Y-AXIS) AND WITH VARIABLE d_0 (X-AXIS) FOR THREE SITES WITH MORE THAN 1 SENSOR ABOVE H_c. THE TEXT FOR EACH PANEL SHOWS THE SLOPE OF THE X~Y RELATIONSHIP (INDICATED WITH A BLUE LINE), AND THE r^2 OF THAT RELATIONSHIP

3. At sites with more than 1 wind speed sensors above H_c, the relationship between z_{0m} and d_0 is calculated. It can be seen in Figure S4, that while a relationship between d_0 and z_{0m} is evident, it doesn't explain a lot of the variance in the two parameters. This may be due to a variation of β, which features in Equation (22).

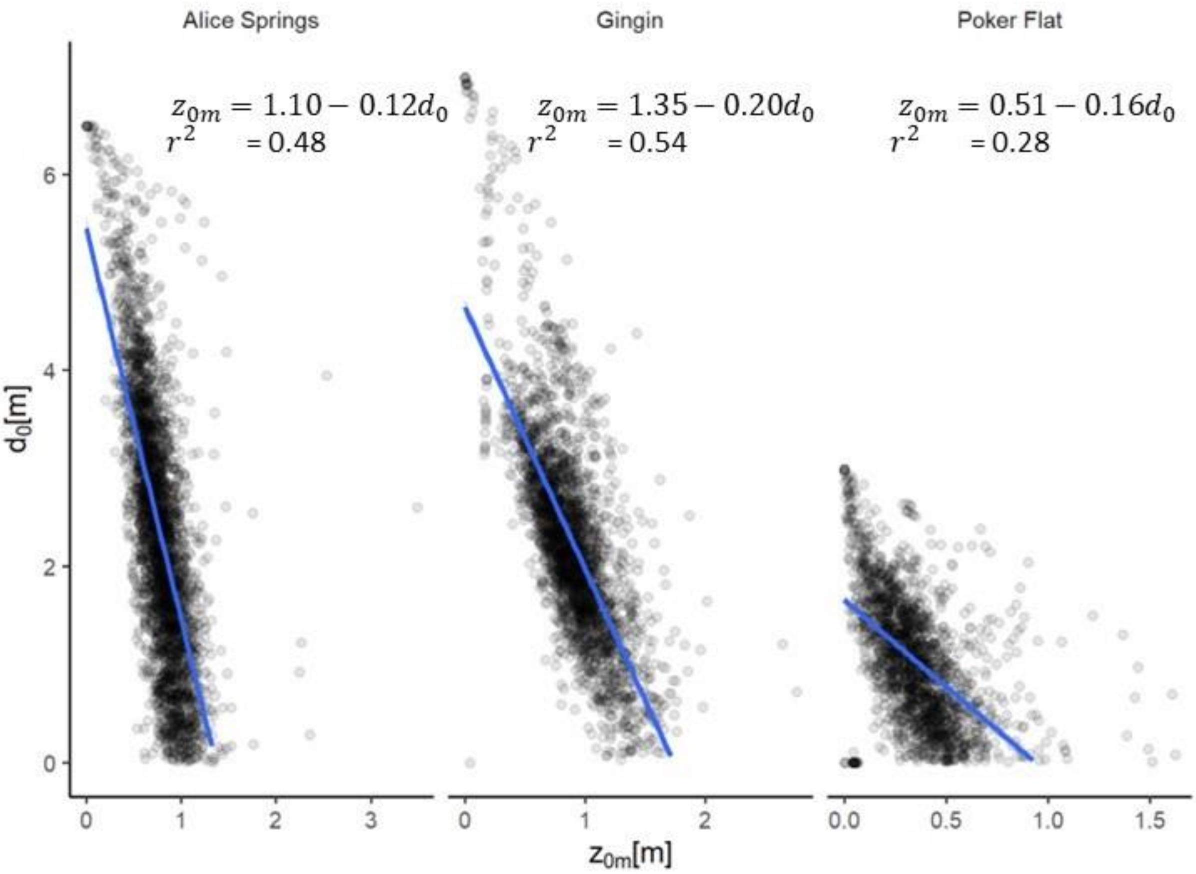

FIGURE S4: RELATIONSHIP BETWEEN D0 AND Z0M AT SITES WHERE THEY ARE CALCULATED SIMULTANEOUSLY GIVEN BY THE EQUATIONS AND THE r^2 VALUES ASSOCIATED WITH THAT RELATIONSHIP

S4 – DATE RANGE OF DATA IN THE STUDY

Site	Start	End
Alice Springs	Jan 2012	Dec 2019
Yanco	Jan 2014	Oct 2020
Gingin	Jan 2015	Dec 2019
Poker Flat	Nov 2010	Dec 2016
Willow Creek <2007	Aug 1999	Nov 2006
Willow Creek >2010	Dec 2010	Apr 2017
Bartlett	Feb 2017	Apr 2021
Charleston	Mar 2001	Dec 2011

S5 – VARIATION OF MODELS WITH $c_d a H_c$

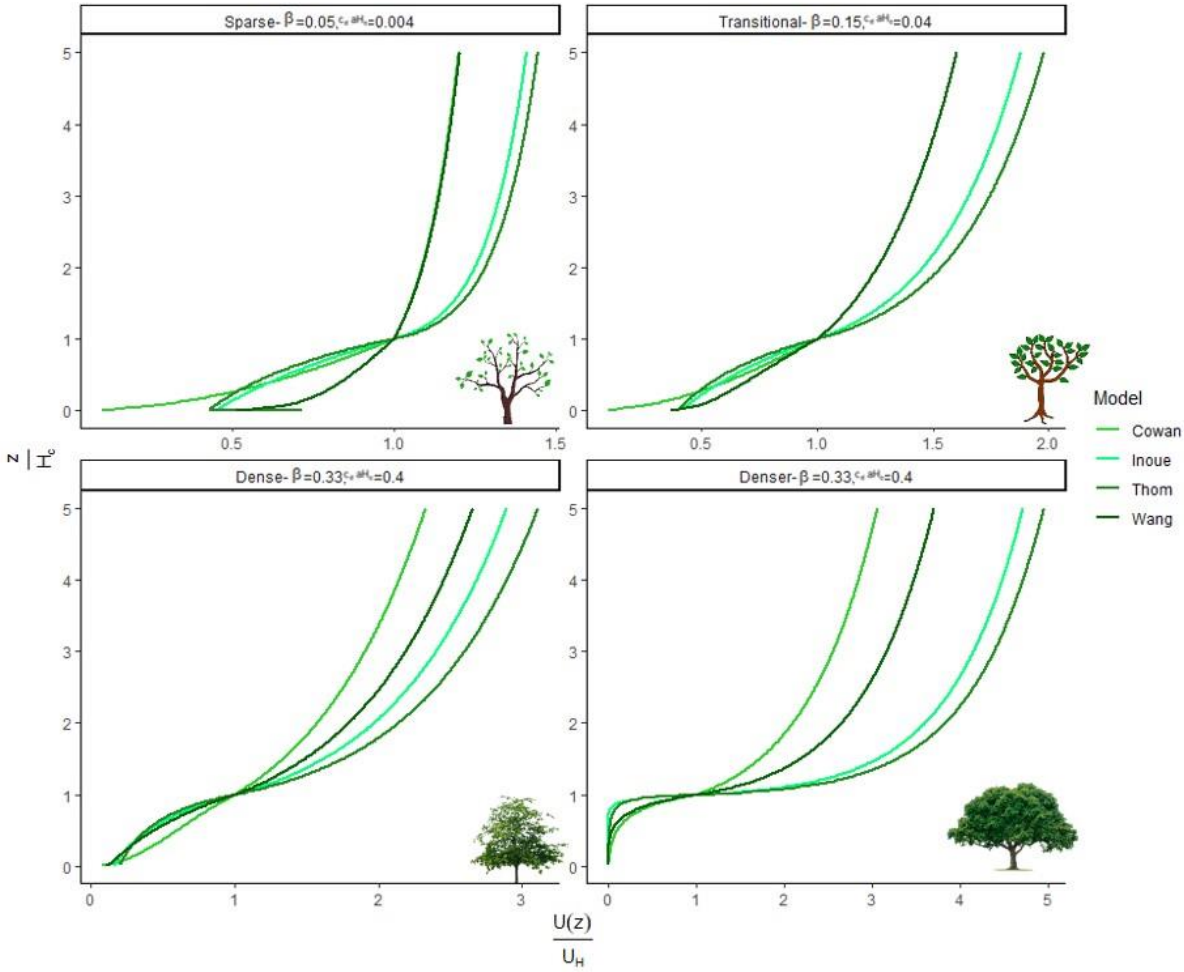

FIGURE S5: THE RESULTS OF THE WIND SPEED MODELS FOR THE GIVEN PARAMETERS WITHIN THE CSL AND UPTO 4 $\mathbf{H_c}$ IN THE ISL FOR THE FOUR MODELS AND FOR FOUR SETS OF $\boldsymbol{\beta}$ AND $\mathbf{c_d a H_c}$.

S6 – z_{0m} THEORETICAL RESULTS

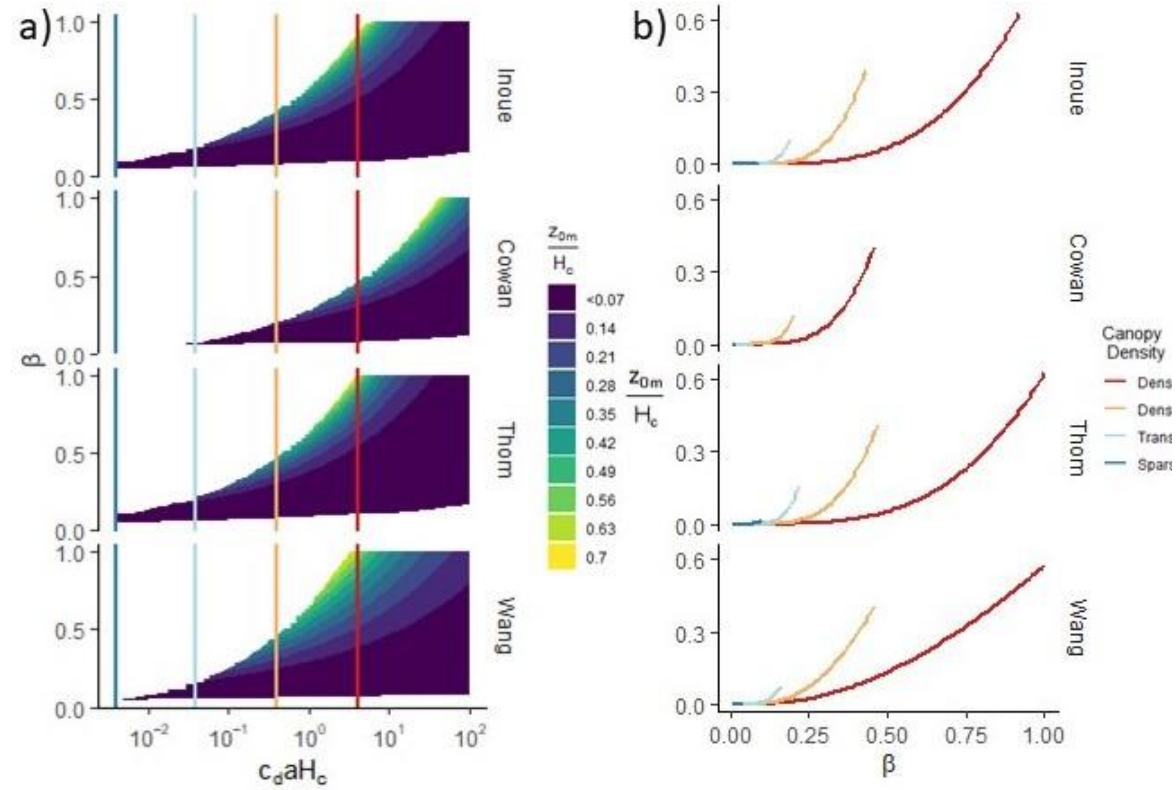

FIGURE S6: THE VARIATION OF z_{0m}/H_c AS FUNCTIONS OF THE TWO NON-DIMENSIONAL PARAMETERS β AND $c_d a H_c$ WITH VALUES GENERATED USING THE 4 DIFFERENT MODELS DISPLAYED AS A) THE CHANGE IN COLOURS FOR DIFFERENT VALUES OF β (Y-AXIS) AND $c_d a H_c$ (LOG X-AXIS) CONTOUR PLOTS FOR THE FOUR MODELS SELECTED IN THE PAPER. THE DIFFERENT COLOURED VERTICAL LINES REPRESENT SECTIONS OF DIFFERENT CANOPY DENSITIES INCREASING FROM LOWEST AT DARK BLUE TO HIGHEST AT RED. THESE SECTIONS FROM THE GRAPH ARE THEN PLOTTED IN B) WITH $\BETA$ ON THE X-AXIS AND THE VALUE OF z_{0m}/H_c ON THE Y-AXIS FOR THE FOUR DIFFERENT CANOPY DENSITIES THAT WERE DISPLAYED TAKEN FROM A).

S7 – DISTRIBUTION OF INVALID VALUES

Site	Good	Upper	Lower	Method
Alice Springs	3211	9	761	NLS
Yanco	799	1069	702	
Gingin	2756	0	54	
Poker Flat	1446	2	630	
Willow Creek	61506	3137	7207	Numerical
Bartlett	2711	7	417	
Charleston	4388	471	104	

S8 – z_{0m} EMPERICAL VARIATION

The empirical results of z_{0m} are presented graphically in Figure S7. The scale here, however, is fixed across different sites between 0 to 5 m. This is because z_{0m} doesn't represent a simple vertical translation in the log profile like d_0, but rather changes the shape of the profile, extracting greater momentum from the fluid flow above it for greater values of z_{0m}. Therefore, the representation of the absolute change is more important than the change with reference to a given height H_c.

The deciduous dense canopies produce a standard deviation of less than 1m. The Charleston and Willow Creek 2 sites z_{0m} means lie in between the conventional (upper) and Raupach (lower) estimates. However, they are within one standard deviation of the Charleston mean but not the Willow Creek 2 mean. The standard deviation of the deciduous transitional species is again the largest in the given set and the conventional assumption of $0.12H_c$ gives estimates within 1 standard deviation of the mean. The evergreen sparse canopies give small standard deviations and their means are quite well predicted by the conventional assumption $0.12H_c$. The grassland site gives a very low estimate indicating a smooth surface, and a low standard deviation as well.

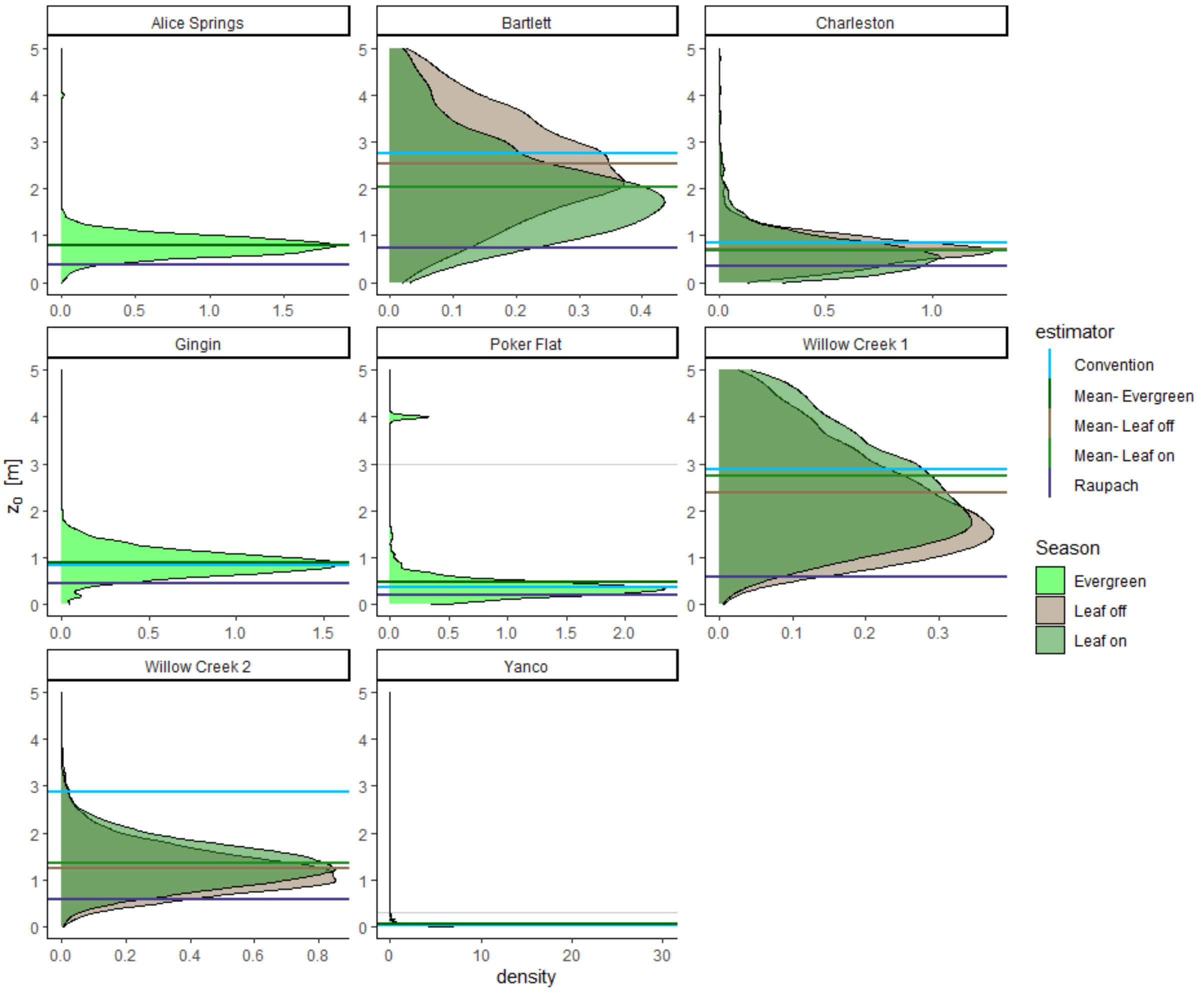

FIGURE S7: DISTRIBUTION OF z_{0m} FOR DIFFERENT SITES. THE Y AXIS REPRESENTS THE VALUE OF z_{0m} [M] SCALED UNIFORMLY ACROSS ALL THE PANELS. THESE ARE SCALED TO THE BE 0 TO 5 METERS FOR EACH SITE. THE X AXIS REPRESENTS THE PROBABILITY DENSITY. THE COLOURS REPRESENT WHETHER THE CANOPIES ARE EVERGREEN OR DECIDUOUS, AND THE SEASON IN CASE THEY ARE DECIDUOUS. THE LIGHT BLUE HORIZONTAL LINE REPRESENTS THE CONVENTION OF $0.12\ H_c$ AND THE DARK BLUE LINE IS THE RAUPACH ASSUMPTION OF z_{0m}. THESE ARE GIVEN ALONGSIDE THE MEANS FOR EACH OF THE PROBABILITY DENSITY FUNCTIONS.

The standard deviation for the majority of the estimates is close to half the mean of the empirical estimate. This is taken to be reason enough to concur with the literature that postulates the variation of d_0 and z_{0m} at a site.

S9 – OBSERVATIONS OF β

The nondimensional variable β was computed for each site and season, with PDFs provided. At all sites, β showed non-trivial variability, consistent with its hypothesized role in causing variability in d_0. At most sites, at least some of the observed values of β exceeded the 0.33. In the dense deciduous sites Charleston and Willow Creek 2, fewer than 50% of the observed β values are lower than 0.3 (see **Error! Reference source not found.**).

FIGURE S8: PROBABILITY DENSITY FUNCTION OF $\boldsymbol{\beta}$ MEASURED AT DIFFERENT SITES AND SEASONS. THE VERTICAL LINE REPRESENTS $\boldsymbol{\beta = 1/3}$ WHICH IS ESTIMATED TO BE ITS MAXIMUM THEORETICAL VALUE.

S10 – PDFS OF $c_d aH_c$

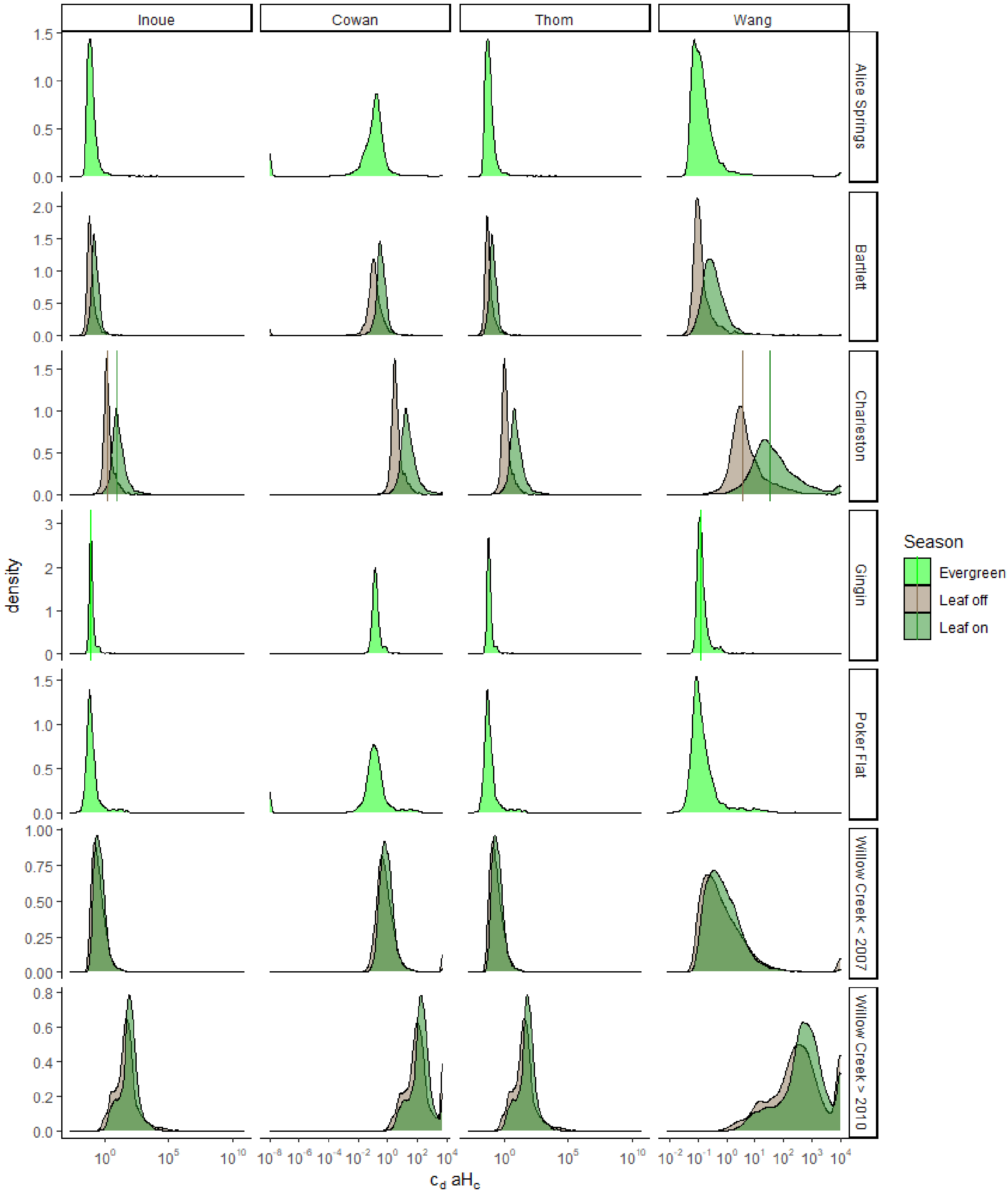

FIGURE S9: $c_d aH_c$ VALUES FOR THE SITES FOR DIFFERENT MODELS AND SEASONS

S11 – RELATIONSHIP BETWEEN d_0/H_c AND β

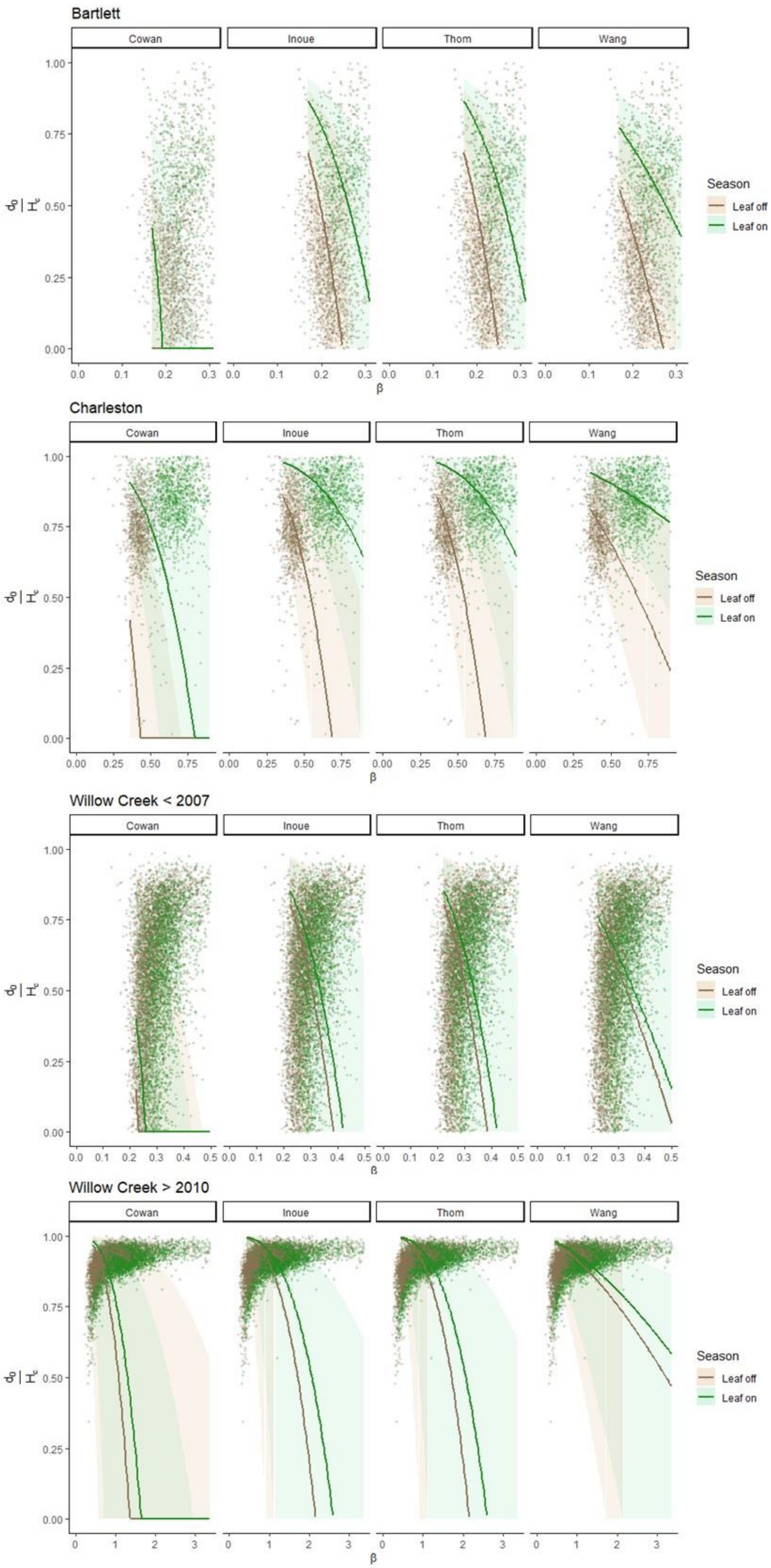
Bartlett
Charleston
Willow Creek < 2007
Willow Creek > 2010
Cowan
Inoue
Thom
Wang
β
Season
Leaf off
Leaf on

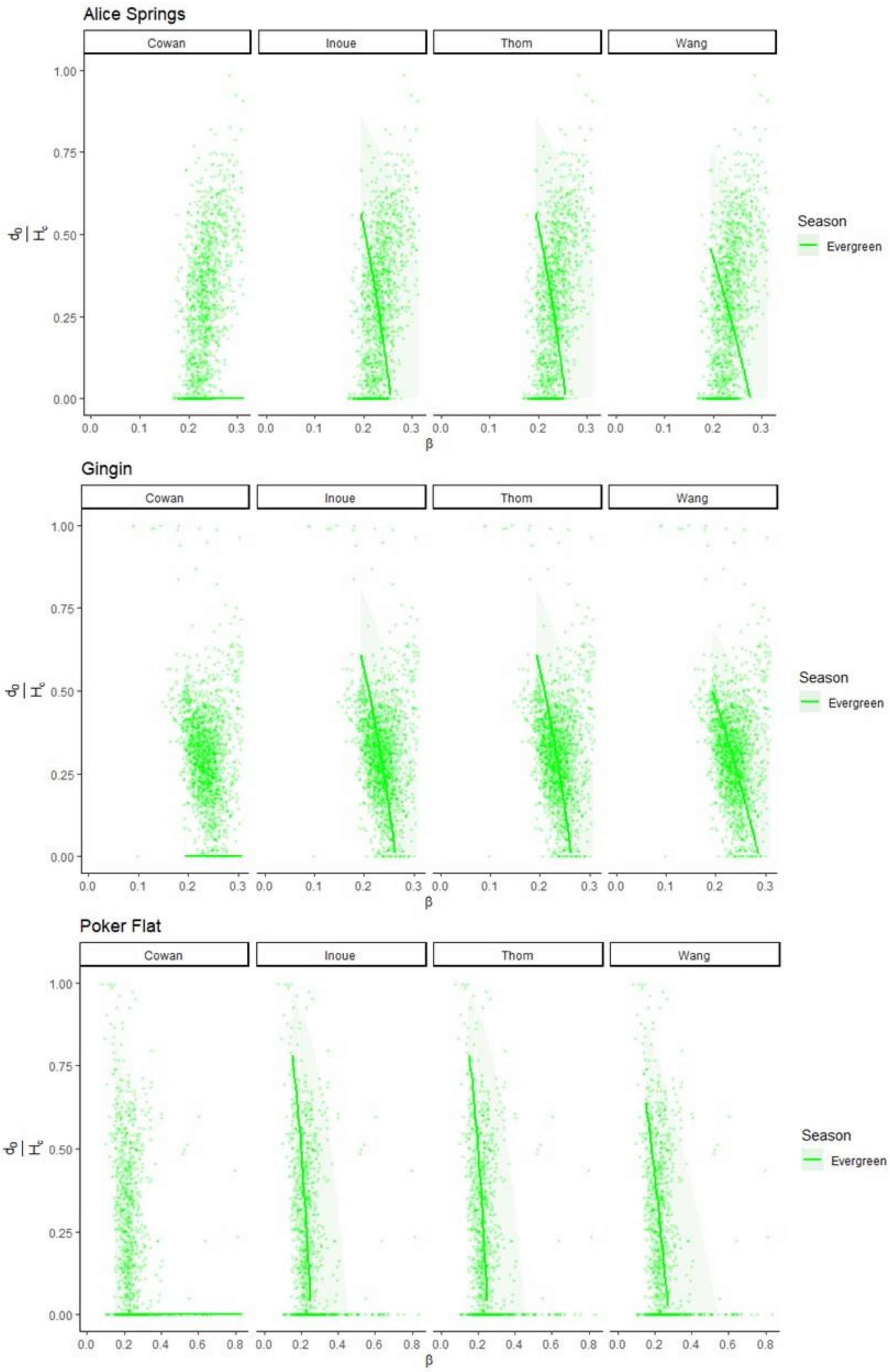

FIGURE S10: THE DISTRIBUTION OF MEASURED β (X-AXIS) AND EMPIRICALLY ESTIMATED d_0/H_c SHOWN BY POINTS. THE LINES INDICATE THE MODELS PREDICTED VALUE OF d_0/H_c FOR GIVEN β USING THE CHOSEN MEDIAN VALUE OF $c_d a H_c$ INDICATED BY THE SOLID LINE, AND THE 10TH AND 90TH PERCENTILE SHOWN AS THE SHADED REGIONS

S12 – USING THE ANALYTICAL VELOCITY FUNCTIONS

The utility of the median value of can be looked at in the intended use of the analytical CSL velocity models, i.e. estimating the U at various z within the CSL. For this assessment the median values of $c_d a H_c$ are used with the measured values of β in the equations (22), (24), (26), and (28), to estimate $U(z)$ within the CSL for the three selected sites presented on the y axis. This is compared with the observed wind speed on the x axis. The same figure for all the sites is given in the supplementary material. In Cowan and Thom, a measurement of d_0/H_c was required to estimate the velocity in the canopy as well, as is shown in equations (24) and (26), and this was used from the empirically estimated d_0/H_c.

The results in Figure S11 show that the models generally do a poor job of predicting the wind velocity within a canopy. For Bartlett, the momentum absorbed by the canopy is underestimated. Therefore, the predicted velocities are higher across the four models, as can be seen by the scatter plot populating the region above the 1:1 line for both seasons. This is more pronounced in the lower canopy (as can be seen by the distance from the 1:1 for the $\frac{z}{H_c} = 0.67$ compared to $\frac{z}{H_c} = 0.83$ at Bartlett), as the underestimation of the momentum extracted by the canopy accumulates, i.e. there is more momentum that should've been extracted by a higher $c_d a$ and going down the canopy height this 'extra unextracted' momentum keeps accumulating. This effect is exacerbated for the leaf off season, as the $c_d a H_c$ is even lower than the erroneous low initial estimate.

For Charleston, the problem is the opposite as there is an overestimation of the momentum extracted by the canopy. Therefore, the models regularly predict the velocity to be considerably lower than the velocity that is measured as is shown by the scatter plot populating the region below the 1:1 line. The leaf off season here has an ameliorating effect, where the overestimation of the momentum extracted by a high value for $c_d a H_c$ is reduced. As the height of measurement is low at Charleston and there is a high $c_d a H_c$, according to the models all the momentum has been extracted from the wind as can be seen in the densest panel in Figure S5.

Gingin scatter plot is the closest to the 1:1 line. At the low height of $\frac{z}{H_c} = 0.27$ the Cowan and Wang models perform the best (Wang being especially formulated with sparse canopies in mind). Inoue and Thom may overestimate the velocity because of their lower boundary condition is not met in the sparse canopies as can be seen in Figure S5's sparse panel.

The model comparison shows the values predicted by Inoue are more scattered than the others. Wang on the other hand, gives a compact distribution as can be seen especially for the Bartlett panels. In all, the median $c_d a H_c$ estimated by using d_0/H_c and β the analytical CSL models are seldom able to recreate reality within the CSL. Their moderate success at Gingin, given that they have been calibrated using the wind profile above the canopy is commendable.

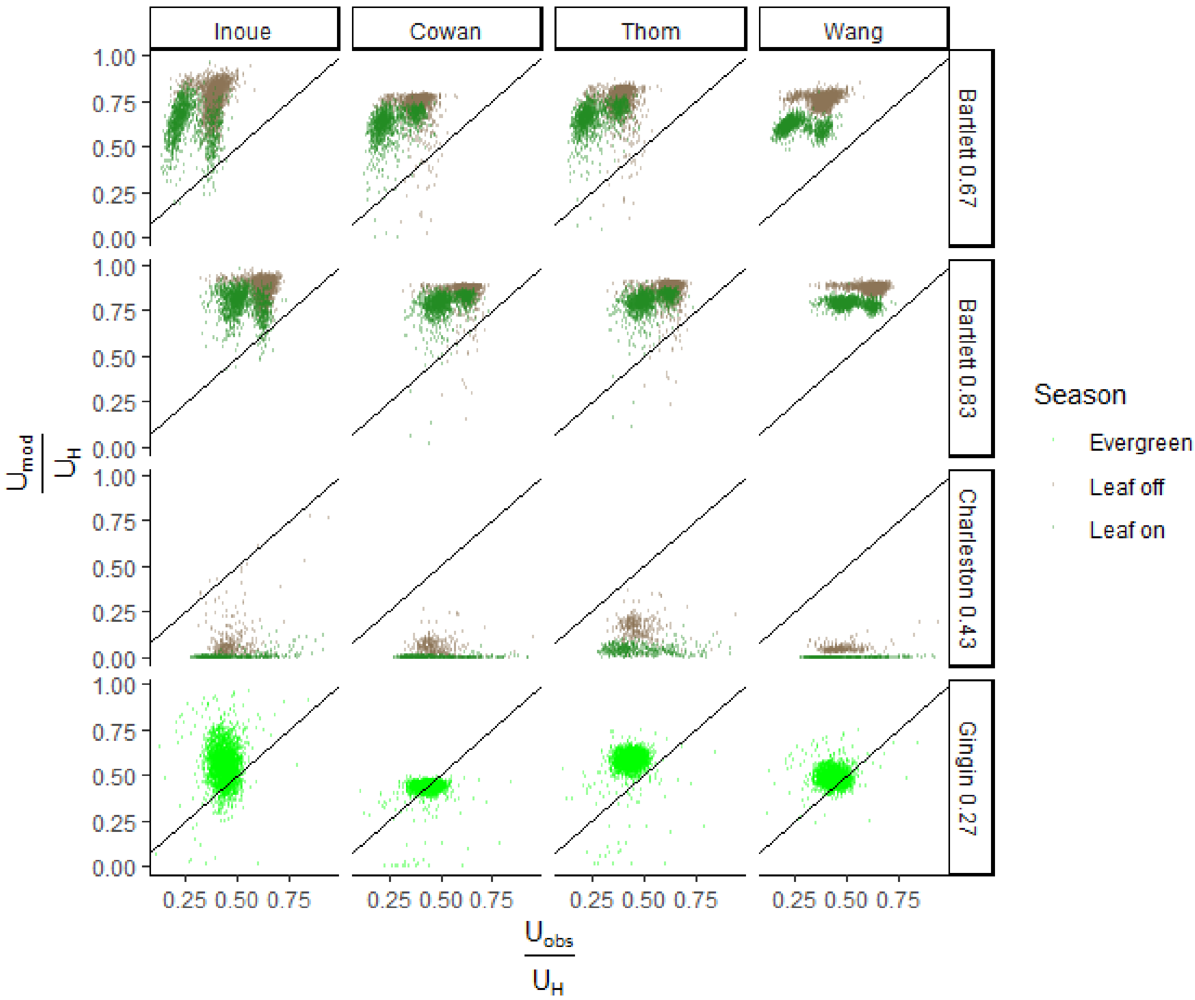

FIGURE S11: THE WIND VELOCITY MEASURED WITHIN THE CANOPY SCALED BY U_H PLOTTED WITH THE VELOCITY PREDICTED BY THE MODELS USING β MEASURED AT THE TIME STEPS. THE BLACK LINE IS THE 1:1 LINE.

S13 – EMPIRICAL d_0 VS ACTUAL PDF

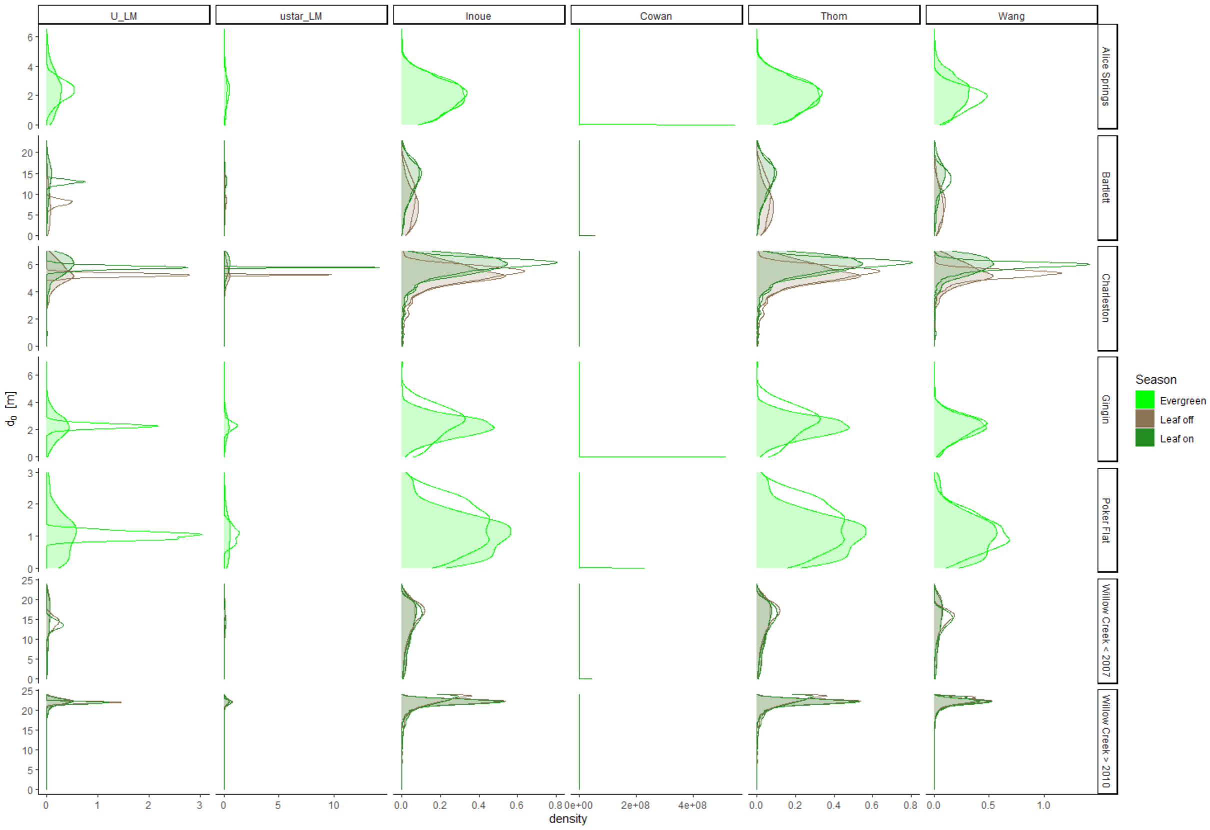

FIGURE S12: PREDICTION OF VARIATION OF d_0 (IN METERS ON THE Y-AXIS) USING VARIOUS THEORIES. THE SHADED AREA IS THE EMPIRICALLY CALCULATED d_0 AND THE LINE IS SHOWING THE DISTRIBUTION PREDICTED BY THE MODEL.

S14 – Performance of d_0 for half an hour predictions

Site	Season	variable	R^2	Adj R^2	rmse	int	slp
Gingin	Evergreen	U	0.04	0.04	0.08	2.22	0.02
		ustar	0.13	0.13	0.23	2.07	0.08
		Inoue	0.12	0.12	1.12	1.46	0.46
		Cowan	0.03	0.03	0.20	-0.07	0.04
		Thom	0.12	0.12	1.12	1.46	0.46
		Wang	0.07	0.07	0.84	1.64	0.25
Alice Springs	Evergreen	U	0.27	0.27	0.57	1.71	0.26
		ustar	0.35	0.35	0.62	1.52	0.34
		Inoue	0.07	0.07	1.01	2.47	-0.24
		Cowan	0.00	0.00	0.16	-0.01	0.01
		Thom	0.07	0.07	1.01	2.47	-0.24
		Wang	0.12	0.12	0.73	2.25	-0.24
Charleston	Leaf off	U	0.00	0.00	0.02	5.14	0.00
		ustar	0.04	0.04	0.18	4.97	0.03
		Inoue	0.01	0.01	1.18	5.31	-0.09
		Cowan	0.00	0.00	1.33	1.52	-0.09
		Thom	0.01	0.01	1.18	5.31	-0.09
		Wang	0.02	0.02	0.71	5.70	-0.11
	Leaf on	U	0.07	0.07	0.23	5.35	0.06
		ustar	0.00	0.00	0.03	5.69	0.00
		Inoue	0.00	0.00	1.06	5.85	-0.07
		Cowan	0.01	0.01	1.85	4.33	-0.19
		Thom	0.00	0.00	1.06	5.85	-0.07
		Wang	0.00	0.00	0.44	6.06	-0.01
Willow Creek < 2007	Leaf on	U	0.05	0.05	0.95	13.09	0.04
		ustar	0.17	0.17	2.01	11.37	0.16
		Inoue	0.13	0.13	4.26	17.81	-0.31
		Cowan	0.01	0.01	3.45	0.27	0.05
		Thom	0.13	0.13	4.26	17.81	-0.31

		Wang	0.17	0.17	2.80	17.03	-0.23
	Leaf off	U	0.06	0.06	1.39	12.98	0.06
		ustar	0.18	0.18	2.12	11.42	0.17
		Inoue	0.13	0.13	4.35	17.80	-0.30
		Cowan	0.02	0.02	3.52	-0.31	0.09
		Thom	0.13	0.13	4.35	17.80	-0.30
		Wang	0.17	0.17	2.94	16.99	-0.23
Willow Creek > 2010	Leaf off	U	0.06	0.06	0.29	20.71	0.05
		ustar	0.17	0.17	0.53	18.29	0.16
		Inoue	0.10	0.10	3.17	36.68	-0.71
		Cowan	0.13	0.13	7.61	57.54	-1.95
		Thom	0.10	0.10	3.17	36.68	-0.71
		Wang	0.11	0.11	2.26	33.20	-0.53
	Leaf on	U	0.04	0.04	0.25	20.74	0.05
		ustar	0.18	0.18	0.43	17.48	0.20
		Inoue	0.11	0.11	3.27	46.16	-1.14
		Cowan	0.19	0.19	6.97	88.28	-3.36
		Thom	0.11	0.11	3.27	46.16	-1.14
		Wang	0.14	0.14	1.86	37.85	-0.73
Bartlett	Leaf off	U	0.01	0.01	0.63	7.86	0.01
		ustar	0.10	0.10	1.44	7.31	0.10
		Inoue	0.03	0.03	4.51	6.86	0.20
		Cowan	0.02	0.02	0.00	0.00	0.00
		Thom	0.03	0.03	4.51	6.86	0.20
		Wang	0.01	0.01	3.47	6.03	0.08
	Leaf on	U	0.11	0.11	1.89	10.31	0.13
		ustar	0.26	0.26	2.28	8.67	0.27
		Inoue	0.01	0.01	4.88	13.03	-0.11
		Cowan	0.02	0.02	1.31	-0.27	0.04
		Thom	0.01	0.01	4.88	13.03	-0.11

		Wang	0.00	0.00	3.17	12.14	-0.04
Poker Flat	Evergreen	U	0.03	0.03	0.13	1.00	0.04
		ustar	0.14	0.14	0.22	0.89	0.14
		Inoue	0.07	0.07	0.67	1.10	0.29
		Cowan	0.00	0.00	0.24	0.03	0.01
		Thom	0.07	0.07	0.67	1.10	0.29
		Wang	0.05	0.05	0.53	0.93	0.19

S15 – PERFORMANCE OF z_{0m} MODELS HALF AN HOUR PREDICTIONS

Site	Season	variable	R^2	Adj R^2	rmse	int	slp
Gingin	Evergreen	U	0.01	0.01	0.01	0.90	0.00
		ustar	0.11	0.11	0.06	0.83	0.07
		Inoue	0.27	0.27	0.58	-0.11	1.31
		Cowan	0.17	0.17	0.32	0.86	0.52
		Thom	0.27	0.27	0.58	-0.11	1.31
		Wang	0.22	0.21	0.46	0.22	0.89
Alice Springs	Evergreen	U	0.02	0.02	0.02	0.77	0.01
		ustar	0.13	0.13	0.09	0.68	0.13
		Inoue	0.02	0.02	0.65	0.76	0.42
		Cowan	0.00	0.00	0.36	1.20	0.08
		Thom	0.02	0.02	0.65	0.76	0.42
		Wang	0.00	0.00	0.50	0.90	0.15
Charleston	Leaf off	U	0.00	0.00	0.04	0.75	0.00
		ustar	0.04	0.04	0.07	0.73	0.03
		Inoue	0.02	0.02	0.69	0.78	0.22
		Cowan	0.03	0.03	0.81	2.18	0.34
		Thom	0.02	0.02	0.69	0.78	0.22
		Wang	0.01	0.01	0.48	0.73	0.09
	Leaf on	U	0.08	0.08	0.15	0.66	0.08
		ustar	0.00	0.00	0.02	0.71	0.00
		Inoue	0.01	0.01	0.65	0.80	0.12
		Cowan	0.00	0.00	0.89	1.81	-0.07
		Thom	0.01	0.01	0.65	0.80	0.12
		Wang	0.02	0.02	0.34	0.51	0.08
Willow Creek < 2007	Leaf on	U	0.00	0.00	0.05	2.75	0.00
		ustar	0.15	0.15	0.43	2.38	0.13
		Inoue	0.01	0.01	0.90	1.85	0.07
		Cowan	0.37	0.37	1.02	0.90	0.73
		Thom	0.01	0.01	0.90	1.85	0.07

		Wang	0.00	0.00	0.79	2.19	0.04
	Leaf off	U	6.08E-05	0.00	0.04	2.43	0.00
		ustar	0.11	0.11	0.38	2.17	0.11
		Inoue	0.01	0.01	0.89	1.73	0.06
		Cowan	0.23	0.22	1.16	1.12	0.68
		Thom	0.01	0.01	0.89	1.73	0.06
		Wang	0.00	0.00	0.78	2.02	0.03
Willow Creek > 2010	Leaf off	U	0.01	0.01	0.04	1.22	0.01
		ustar	0.17	0.17	0.20	1.02	0.17
		Inoue	0.02	0.02	0.93	1.34	-0.24
		Cowan	0.01	0.01	1.22	1.69	-0.25
		Thom	0.02	0.02	0.93	1.34	-0.24
		Wang	0.02	0.02	0.79	1.43	-0.21
	Leaf on	U	0.01	0.01	0.06	1.33	0.01
		ustar	0.18	0.18	0.20	1.09	0.19
		Inoue	0.02	0.02	0.99	1.69	-0.32
		Cowan	0.05	0.05	1.22	2.51	-0.58
		Thom	0.02	0.02	0.99	1.69	-0.32
		Wang	0.02	0.02	0.78	1.68	-0.26
Bartlett	Leaf off	U	0.06	0.06	0.19	2.48	0.04
		ustar	0.04	0.04	0.20	2.45	0.04
		Inoue	0.48	0.48	0.69	0.24	0.81
		Cowan	0.52	0.52	0.44	1.82	0.59
		Thom	0.48	0.48	0.69	0.24	0.81
		Wang	0.45	0.44	0.66	0.75	0.68
	Leaf on	U	0.00	0.00	0.08	2.07	0.00
		ustar	0.09	0.09	0.42	1.83	0.11
		Inoue	0.14	0.14	0.96	1.01	0.41
		Cowan	0.19	0.18	0.58	2.51	0.37
		Thom	0.14	0.14	0.96	1.01	0.41

		Wang	0.15	0.15	0.84	1.29	0.36
Poker Flat	Evergreen	U	0.00	0.00	0.00	0.37	0.00
		ustar	0.14	0.14	0.12	0.32	0.13
		Inoue	0.44	0.44	0.40	-0.25	2.08
		Cowan	0.51	0.51	0.23	0.30	0.64
		Thom	0.44	0.44	0.40	-0.25	2.08
		Wang	0.41	0.40	0.33	-0.10	1.54

S16 –THE EFFECTS OF CHANGING AERODYNAMIC PROPERTIES ON WIND SPEED

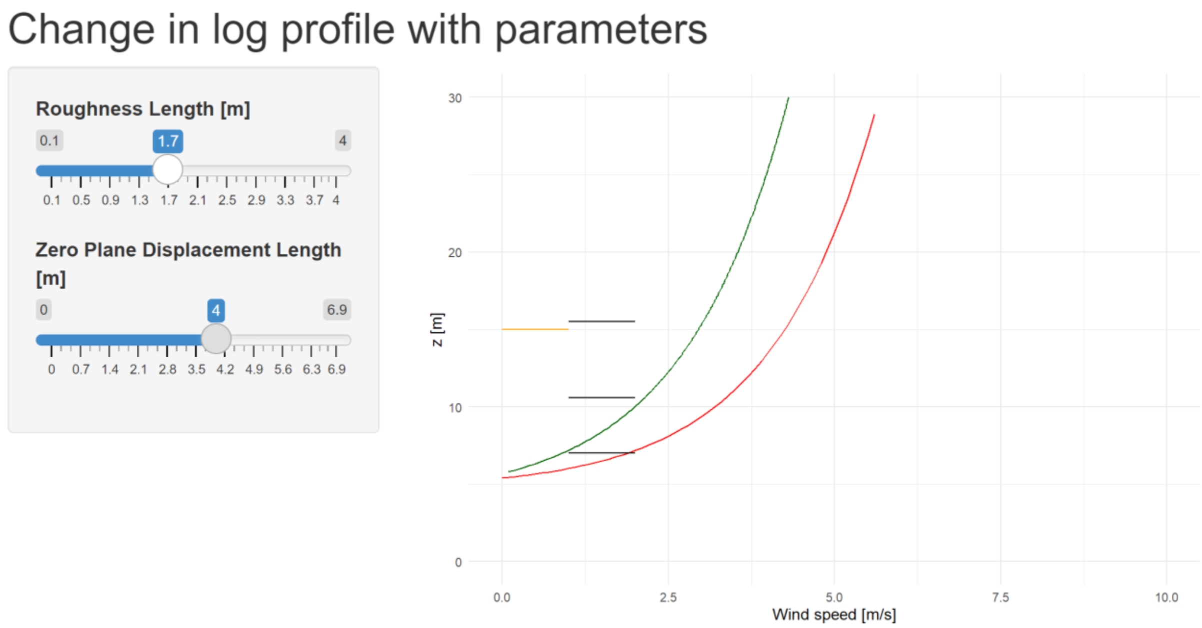

FIGURE S13: SHINY APP DEMONSTRATING THE EFFECT OF INCORRECT ESTIMATION OF AERODYNAMIC CHARACTERISTICS OF A SURFACE ON WIND PROFILE ESTIMATION

S17 –EFFECTS OF AERODYNAMIC PROPERTIES ON POTENTIAL EVAPORATION

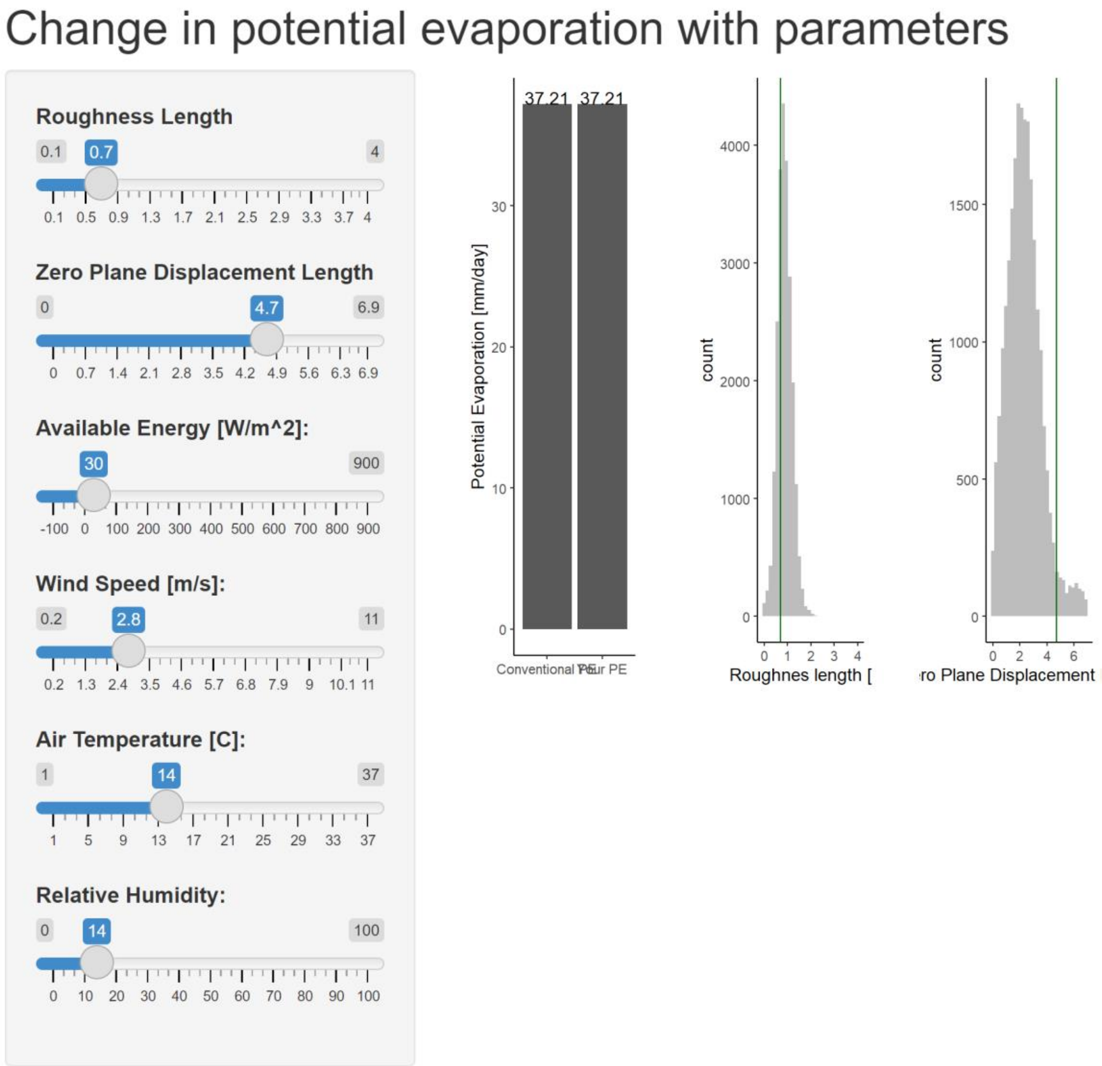

FIGURE S14: EFFECT OF CHANGING AERODYNAMIC CHARACTERISTICS ON POTENTIAL EVAPORATION